The intrinsically disordered TC-1 interacts with Chibby via regions with high helical propensity

CHRIS GALL, HANYU XU, ANNE BRICKENDEN, XUANJUN AI, AND WING YIU CHOY

Department of Biochemistry, University of Western Ontario, London, Ontario N6A 5C1, Canada

(RECEIVED June 7, 2007; FINAL REVISION August 2, 2007; ACCEPTED August 10, 2007)

Abstract

Thyroid cancer 1 (TC-1) is a 106-residue naturally disordered protein that has been found to associate with thyroid, gastric, and breast cancers. Recent studies showed that the protein functions as a positive regulator in the Wnt/β-catenin signaling pathway, a pathway that is known to play essential roles in developmental processes and causes tumor formation when misregulated. By competing with β-catenin for binding to Chibby (Cby), a conserved nuclear protein that antagonizes the β-catenin–mediated transcriptions, TC-1 up-regulates a number of β-catenin target genes that are known to be involved in the aggressive behavior of cancers. In order to gain a molecular understanding of the role TC-1 plays in regulating the Wnt/β-catenin signaling pathway, detailed structural studies of the protein and its interaction with Cby are essential. In this work, we used nuclear magnetic resonance (NMR) spectroscopy to elucidate the structure of TC-1 and its interaction with Cby. Our results indicate that even though TC-1 is naturally disordered, the protein adopts fairly compact conformations under nondenaturing conditions. Chemical shift analysis and relaxation measurements show that three regions (D44-R53, K58-A64, and D73-T88) with high-helical propensity are present in the C-terminal portion of TC-1. Upon addition of Cby, significant broadening of resonance signals derived from these helical regions of TC-1 was observed. The result indicates that the intrinsically disordered TC-1 interacts with Cby via its transient helical structure.

Keywords: thyroid cancer 1 (TC-1); Chibby (Cby); nuclear magnetic resonance; disordered protein; Wnt/β-catenin signaling pathway; cancers

Supplemental material: see www.proteinscience.org

Since its first identification as a novel gene highly expressed in thyroid cancer (Chua et al. 2000), *thyroid cancer 1* (*TC-1*) has subsequently been found to be involved also in gastric (Kim et al. 2003) and breast (Yang et al. 2006) cancers. Recently, Lee and his coworkers discovered that TC-1 functions as a positive regulator in the Wnt/β-catenin signaling pathway (Jung et al. 2006), a pathway that is known to play essential roles in developmental processes and lead to cancers when misregulated (Polakis 2000; Giles et al. 2003). In the absence of a Wnt signal, the cellular concentration of β-catenin is tightly regulated by a multi-protein destruction complex composed of Axin, adenomatous polyposis coli (APC), and glycogen synthase kinase 3β (GSK-3β). To maintain the cytoplasmic β-catenin at a low level, GSK-3β phosphorylates the protein and the product is subsequently ubiquitylated and targeted for degradation by the proteasome. The Wnt signal, on the other hand,

Reprint requests to: Wing Yiu Choy, Department of Biochemistry, University of Western Ontario, London, Ontario N6A 5C1, Canada; e-mail: jchoy4@uwo.ca; fax: (519) 661-3175.

Abbreviations: TC-1, thyroid cancer 1; CD, circular dichroism; Cby, Chibby; TCF, T-cell factor; LEF, lymphoid enhancer factor; NMR, nuclear magnetic resonance; R_1, longitudinal relaxation rate; $R_{1\rho}$, relaxation rate in rotating frame; R_2, transverse relaxation rate; *NOE*, nuclear Overhauser effect.

Article published online ahead of print. Article and publication date are at http://www.proteinscience.org/cgi/doi/10.1110/ps.073062707.

inhibits the activity of the destruction complex and leads to the accumulation of β-catenin in the cytoplasm. The β-catenin is then translocated to the nucleus, where it interacts with the T-cell factor/lymphoid enhance factor (TCF/LEF) transcription factors and regulates the transcription of various target genes (Gordon and Nusse 2006).

The β-catenin–mediated transcription can be negatively regulated by Chibby (Cby), a conserved nuclear protein that competes with TCF/LEF for binding to β-catenin (Takemaru et al. 2003). Based on the primary sequence analysis, the 126-residue Cby is predicted to have a coiled-coil domain in the C-terminal portion of the protein; however, no detailed structural information of this protein is available so far. In vitro pulldown assays demonstrated that Cby directly binds to the C-terminal region of β-catenin via its C-terminal half (residues 64–126). On the other hand, TC-1 can compete with β-catenin for binding to Cby and relieves the antagonistic activity of Cby on the β-catenin–mediated transcription, leading to the up-regulation of many cancer-associated genes such as *LAMC2*, *MMP-7*, *MMP-14*, *CCND1*, *c-Met*, and *CD44* (Jung et al. 2006). This agrees with the clinical finding that the expression of TC-1 correlates with the aggressive biological behaviors in gastric cancer (Kim et al. 2006). To gain a better understanding of the regulatory role TC-1 plays in the Wnt/β-catenin signaling pathway and its relationship to cancers, detailed structural studies of this protein and its interaction with Cby are necessary.

Initial characterization of recombinant TC-1 demonstrated that the protein is monomeric but lacks stable secondary and tertiary structure under physiological conditions (Sunde et al. 2004). Even though it is commonly accepted that the functional role of a protein is highly related to its three-dimensional structure, an increasing number of proteins are being identified recently as disordered yet still biologically functional. Importantly, many of these proteins play crucial roles in transcription (Liu et al. 2006) and cell signaling or are involved in cancers (Iakoucheva et al. 2002). Detailed structural studies of this class of proteins are critical for us to understand their roles in cellular processes.

With the recent advances in technology and methodology, nuclear magnetic resonance (NMR) spectroscopy is emerging as a powerful technique for structural and dynamic studies of naturally disordered proteins. In this work, we used NMR spectroscopy to extensively characterize the structure and dynamics of TC-1 and its interaction with Cby. Our results indicate that despite the naturally disordered nature, TC-1 possesses a significant amount of transient structure. Based on the results of chemical shift analysis and relaxation measurements, three regions (D44-R53, K58-A64, and D73-T88) with high-helical propensity present in the C-terminal portion of TC-1 were identified. The chemical shift mapping technique was used to investigate the interaction between TC-1 and Cby. Unlabeled Cby was titrated to the ^{15}N-labeled TC-1, and the structural change of the latter was monitored by ^{1}H-^{15}N HSQC experiments. The result indicates that the transient helical structure present in the disordered TC-1 is crucial for its interaction with Cby.

Results

Backbone assignment and secondary structure propensity analysis

A ^{13}C/^{15}N-labeled TC-1 protein sample was prepared following the purification protocol proposed by Sunde et al. (2004), with modification noted in the Materials and Methods section. Heteronuclear multidimensional NMR experiments were then performed for the backbone chemical shift assignment of the protein. Figure 1 shows the ^{1}H-^{15}N HSQC spectrum of TC-1. The lack of dispersion in amide proton chemical shifts (7.7–8.7 ppm) confirms that TC-1 is disordered under nondenaturing conditions. By using a set of five heteronuclear triple-resonance experiments described in the Materials and Methods section, the $^{1}H_N$, ^{15}N, $^{13}C_\alpha$, $^{13}C_\beta$, and ^{13}CO resonance signals of 75 residues (out of the 105 nonproline residues) in TC-1 were assigned. Even though complete backbone assignment could not be achieved due to the profound signal-overlap problem, useful structural information of the protein can still be extracted. By comparing the observed backbone $^{13}C_\alpha$, $^{13}C_\beta$, and ^{13}CO chemical shifts to the predicted carbon chemical shifts of a random coil, residual structure present in different parts of the protein was determined. To estimate the conformational propensity quantitatively, we have used the program SSP (Marsh et al. 2006) to determine secondary structure propensity of TC-1 in a residue-specific manner. The result is shown in Figure 2. The calculation was based on the observed $^{13}C_\alpha$, $^{13}C_\beta$, and ^{13}CO chemical shifts and the expected chemical shift values of each amino acid type in the α-helix, β-strand, and random-coil conformations of globular proteins (Zhang et al. 2003; Marsh et al. 2006). According to Marsh et al. (2006), the SSP score for each amino acid can be interpreted as the expected fraction of α-helix or β-strand structure. For instance, a SSP score of 0.5 (−0.5) for a given residue reflects that 50% of the structures in the conformational ensemble are helical (β-structure) at that position (Marsh et al. 2006). The calculated SSP scores clearly indicate that even though TC-1 is naturally disordered, the C-terminal portion of the protein has a high-helical propensity, especially in the region between residues D44 and T88. This relatively structured segment

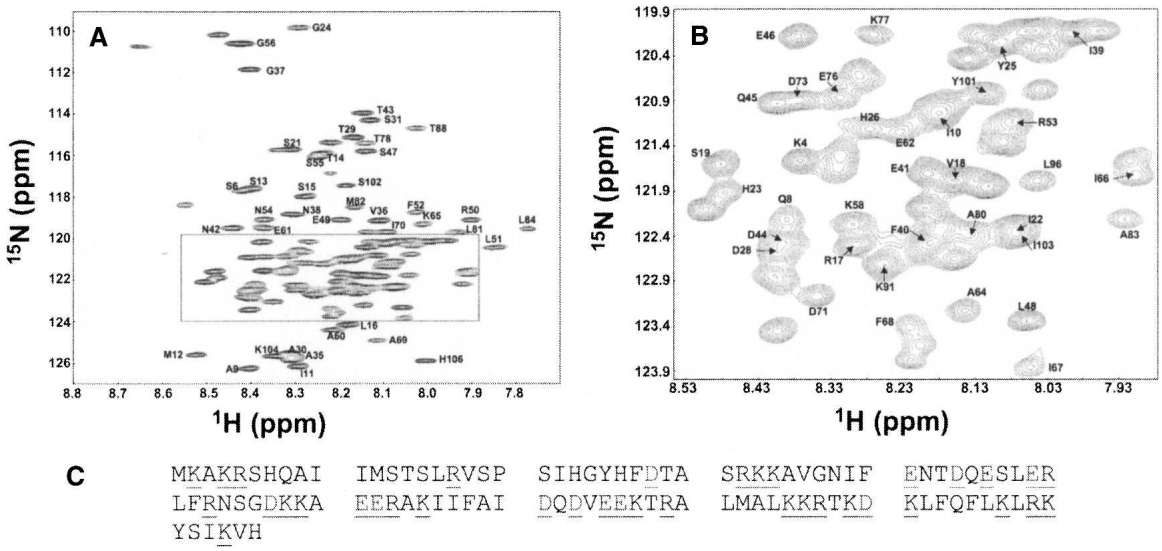

Figure 1. Primary sequence and two-dimensional ^{1}H-^{15}N HSQC spectrum of TC-1 at pH 5.0 and 25°C. The spectrum was recorded at 600 MHz. (*A*) Backbone amide proton resonance signals are crowded in a narrow region (7.7–8.7 ppm). Amide resonances of 75 residues (out of 105 nonproline residues) were assigned. (*B*) Expansion of the squared region of *A* to allow the labeling of peaks in this crowded region. (*C*) The protein sequence of TC-1 with the acidic residues (Asp and Glu) and basic residues (Arg and Lys) underlined.

of TC-1 can be subdivided into three helical regions, D44-R53 (α1), K58-A64 (α2), and D73-T88 (α3), where each residue in these regions has the SSP score >0.2 (Fig. 2). The helical propensity is most pronounced in α3, where nine of the assigned residues show SSP scores >0.7. The result strongly suggests a significant population of the conformers in the disordered ensemble have residues in the α3 region adopt stable helical conformations. The presence of high helical propensity at the C-terminal portion of TC-1 also agrees with the circular dichroism (CD) data reported by Sunde et al. (2004). By using CD spectropolarimetry, Sunde et al. (2004) demonstrated that under nondenaturing conditions (pH 7), the CD signal of TC-1 at ~200 nm is significantly less negative than that of a random coil and negative ellipticity was also observed at ~222 nm, reflecting that the protein is not fully unstructured but has a significant helical content under the conditions used.

Temperature gradients of amide proton chemical shifts

To further characterize the residual structure presence in TC-1, we measured the temperature gradients of the amide proton chemical shifts ($\Delta\delta_{NH}/\Delta T$). The result is shown in Figure 3A. $\Delta\delta_{NH}/\Delta T$ values for 48 residues ranging from −9 ppb/°C to −3 ppb/°C were observed, with only five residues (E46, L48, E49, K77, and L81) displaying $\Delta\delta_{NH}/\Delta T$ slightly larger than −4 ppb/°C. $\Delta\delta_{NH}/\Delta T$ has been widely used as a parameter to estimate the solvent accessibility of amide protons in proteins. Experimental measurements showed that amide protons in random-coil peptides generally have large and negative $\Delta\delta_{NH}/\Delta T$ around −7 ppb/°C (Merutka et al. 1995). For folded proteins, it is commonly accepted that a large and negative $\Delta\delta_{NH}/\Delta T$ indicates the amide proton is solvent exposed, while a less negative or positive $\Delta\delta_{NH}/\Delta T$ (>−4 ppb/°C) suggests that the proton may be sequestered from the solvent (Andersen et al. 1997). For disordered proteins, however, the situation is more complicated. Besides the alteration of hydrogen-bond strength to the solvent upon temperature change, the equilibrium of the disordered state ensemble may also shift toward more

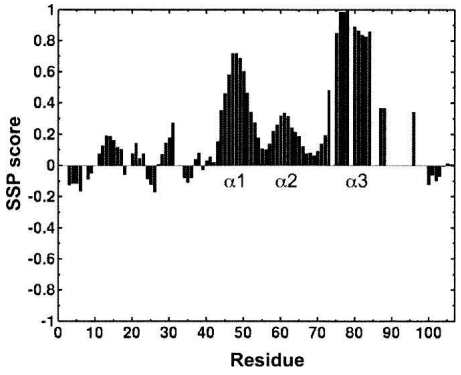

Figure 2. Secondary structure propensity (SSP) scores for TC-1 calculated on the basis of the $^{13}C_{\alpha}$, $^{13}C_{\beta}$, and ^{13}CO chemical shifts using the program SSP (downloaded from http://pound.med.utoronto.ca/software.html) (Marsh et al. 2006). Positive and negative SSP values indicate helical and β-strand propensity, respectively. α1, α2, and α3 represent the three regions with high helical propensity (D44-R53, K58-A64, D73-T88) as mentioned in the text, respectively.

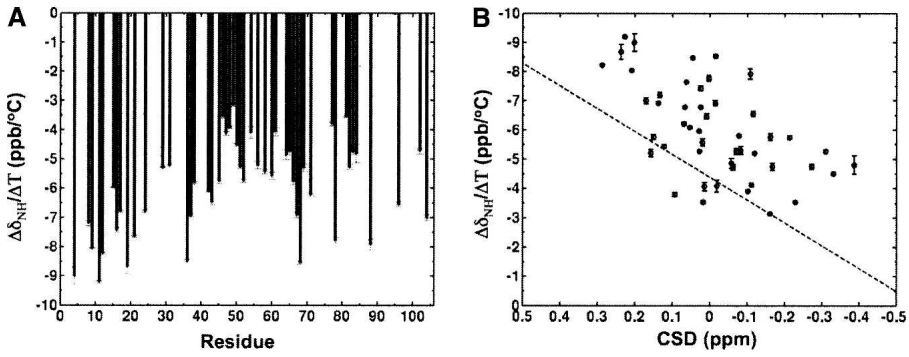

Figure 3. (*A*) The temperature gradients of the amide proton chemical shifts ($\Delta\delta_{NH}/\Delta T$) in TC-1 at pH 5.0. (*B*) The plot of $\Delta\delta_{NH}/\Delta T$ versus the NH chemical shift deviations from random-coil reference values (CSD) in a format proposed by Andersen et al. (1997). The dashed line corresponds to $\Delta\delta_{NH}/\Delta T = -4.4–7.8*(CSD)$.

random-coil conformations when the temperature increases. Both effects contribute to the temperature gradients of amide protons and make the interpretation of $\Delta\delta_{NH}/\Delta T$ data less straightforward (Andersen et al. 1997). Despite the complexity, Andersen et al. (1997) suggested that by plotting $\Delta\delta_{NH}/\Delta T$ versus NH chemical shift deviations from random-coil reference values (CSD), useful structural insights of the polypeptide structure can still be retrieved. Figure 3B shows the plot of $\Delta\delta_{NH}/\Delta T$ versus CSD for TC-1. A correlation coefficient of 0.58 is observed between the temperature gradients and the chemical shift deviations, with a slope of −5.9 ppt/°C. Based on a detailed analysis of $\Delta\delta_{NH}/\Delta T$ for proteins and peptides, Andersen et al. (1997) concluded that if a single structure is dominated in the conformational equilibrium (i.e., with population of 35%–70%), a correlation coefficient larger than 0.7 and a slope more negative than −8 ppt/°C are expected for the plot of $\Delta\delta_{NH}/\Delta T$ versus CSD. Therefore, the disordered state ensemble of TC-1 does not seem to be dominated by a single folded structure in the conformational ensemble. Further, according to Andersen et al. (1997), the dashed line on Figure 3B represents the cutoff line of $\Delta\delta_{NH}/\Delta T = -4.4–7.8*CSD$, which can be used to differentiate sequestered NHs from those that are solvent exposed. For the exposed amide protons, the $\Delta\delta_{NH}/\Delta T$ values are expected to be above the cutoff, while for those that are sequestered, the $\Delta\delta_{NH}/\Delta T$ values should appear below the line (Andersen et al. 1997). Our result suggests that even though there is a significant amount of residual structure present in the protein, most of the amide protons in TC-1 are still exposed to the solvent to some extent.

Hydrodynamic radius measurement of the disordered state ensemble

Since measurement of the average size of the disordered state ensemble can also shed light on the nature of the conformations populated by the protein (Wilkins et al. 1999), we have determined the compactness of the naturally disordered TC-1 using the Pulsed-Field Gradient NMR (PFG-NMR) technique (Altieri et al. 1995). The ensemble-averaged hydrodynamic radius (R_h) of TC-1 under nondenaturing conditions at 25°C was determined to be 26.5 ± 0.5 Å. Using the empirical equations developed by Wilkins et al. (1999), which relate the expected hydrodynamic radius of a globular protein in its native folded state (R_h^N) and fully denatured state (R_h^D) to the number of residues in the polypeptide chain, a folded protein with the same number of residues of TC-1 (including the N-terminal His_6-tag) is predicted to have the R_h^N and R_h^D values of 19.3 and 34.8 Å, respectively. Based on the experimentally measured hydrodynamic radius and these two predicted values, a compaction factor (C), which is defined as $C = \frac{R_h^D - R_h}{R_h^D - R_h^N}$, was calculated (Wilkins et al. 1999). For TC-1 under the nondenaturing conditions used, the disordered state ensemble has a compaction factor of 0.54.

Backbone ^{15}N spin relaxation measurements

The site-specific dynamical information of a disordered protein can be assessed by NMR spin relaxation measurements (Alexandrescu and Shortle 1994; Bracken 2001; Dyson and Wright 2001; Choy et al. 2003). In this work, we have used the backbone ^{15}N longitudinal relaxation rate (R_1), relaxation rate in rotating frame ($R_{1\rho}$), and steady-state ^1H-^{15}N *NOE* experiments to probe the backbone dynamics of individual residues in TC-1. Figure 4 shows the result of backbone ^{15}N relaxation measurements at a magnetic field strength of 14.1 T (^1H frequency of 600 MHz). The transverse relaxation rates (R_2) were calculated on the basis of the measured R_1 and $R_{1\rho}$ values as mentioned in the Materials and Methods section.

With the exception of H106 at the C terminus, the R_1 of all residues fall in a narrow range from 1.4–1.8 s^{-1}.

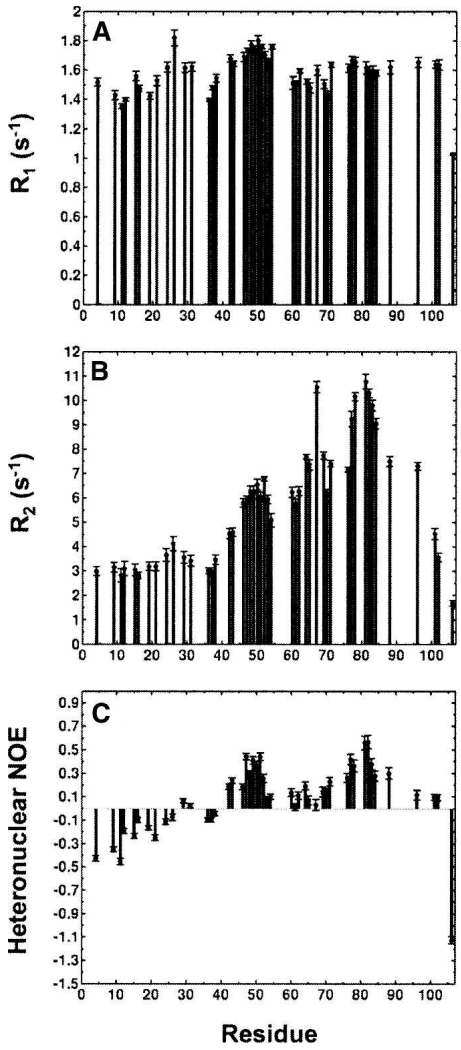

Figure 4. Backbone ^{15}N relaxation measurements of TC-1 at pH 5.0 and 298 K. The data were recorded at 600-MHz field strength. (*A*) Longitudinal relaxation rate (R_1), (*B*) transverse relaxation rate (R_2), and (*C*) steady-state ^{1}H-^{15}N *NOE*.

On the other hand, the R_2, which are more sensitive to the motions on nanosecond and microsecond to microsecond timescales, display a larger variation along the sequence, ranging from 1.7–10.8 s^{-1} (Fig. 4B). For disordered and unfolded proteins, a small R_2 value generally implies the residue is located in a highly flexible segment, while a large R_2 indicates the residue is positioned in a more structured region with limited mobility (Alexandrescu and Shortle 1994; Choy and Kay 2003; Choy et al. 2003). Higher R_2 values (>6 s^{-1}) are observed for most of the residues in the α_1, α_2, and α_3 regions. The result is consistent with the chemical shift analysis that residues in these three regions have high-helical propensity, while the rest of the protein is largely unstructured. This is further supported by the result of ^{1}H-^{15}N *NOE* measurements. For a residue in a folded protein with molecular weight similar to that of TC-1, the maximum *NOE* value should be ~0.83 (assuming the overall tumbling time of the protein is 10 ns). Diminished *NOE* value indicates an increase in the dynamics of the residue on the picosecond–nanosecond timescale. For a highly flexible polypeptide, the *NOE* values observed are usually negative. Figure 4C shows that most of the residues from 4–40 have negative *NOE* values, indicating that the N-terminal portion of the protein is highly unstructured. In contrast, residues in the α_1, α_2, and α_3 regions all display positive values of *NOE*, suggesting these three regions are more restricted in motions on the picosecond–nanosecond timescale.

Interaction of TC-1 with Cby

The chemical shift mapping technique was used to probe the interaction between TC-1 and Cby. Unlabeled Cby was titrated to the ^{15}N-labeled TC-1, and the structural change of the latter was monitored by ^{1}H-^{15}N HSQC experiments (Fig. 5). Due to the limited solubility of Cby (<0.2 mM) under the conditions used, however, saturation of the binding could not be achieved. Upon addition of Cby, significant peak broadening of many resonance signals derived from the C-terminal portion of TC-1 was observed, while signals from the N-terminal part of the protein are largely unperturbed. Residues that display the most significant peak broadening (labeled in Fig. 5A) upon addition of Cby are located mainly in the α1 and α3 regions of TC-1, while some of them are positioned in the linker between α2 and α3. The result strongly suggests that TC-1 interacts with Cby through its transient helical structure. One possible explanation of the observed peak broadening is that, in the presence of Cby, TC-1 undergoes conformational exchange between its free and bound states on the intermediate timescale. However, we are aware that the mechanism of this protein–protein interaction can be more complicated. Due to the potential of coupling between the folding and binding processes, data interpretation can be less straightforward (Sugase et al. 2007). More experiments are needed to scrutinize the mechanism by which TC-1 interacts with Cby, and the thermodynamic details of their binding.

Discussion

Due to the lack of stable tertiary fold, naturally disordered proteins exist as ensembles of distinct conformers in equilibrium under physiological conditions (Choy and Forman-Kay 2001; Dyson and Wright 2004). The structural plasticity of a disordered protein allows it to respond rapidly to the environmental changes and more importantly, to interact with multiple targets by adopting

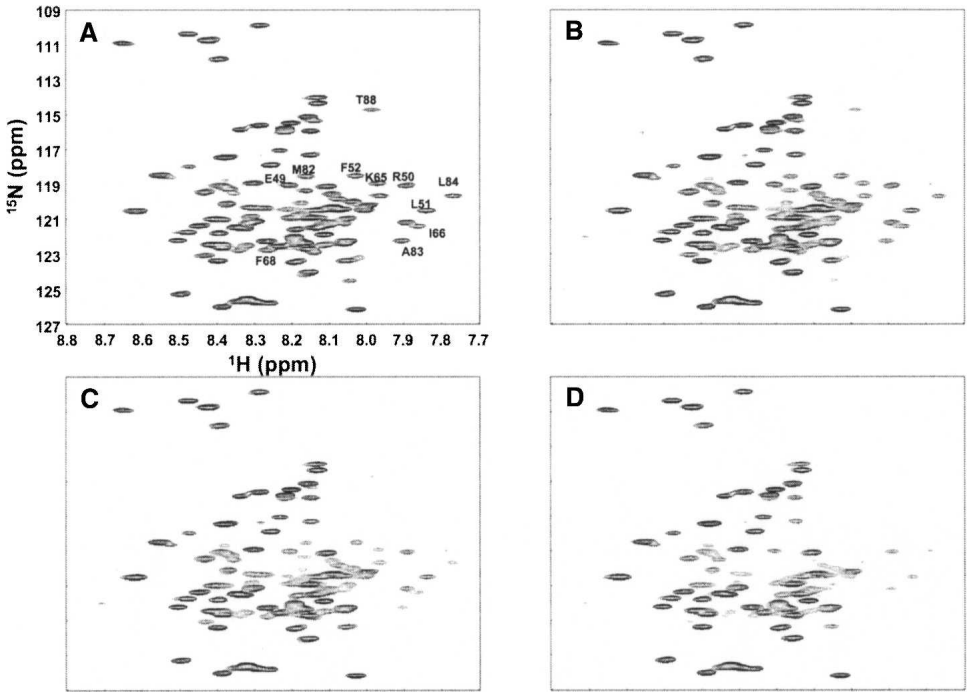

Figure 5. ^{1}H-^{15}N HSQC spectra of 70 μM of ^{15}N-labeled TC-1 (in 10 mM sodium acetate + 100 mM NaCl at pH 5.0) recorded in the presence of (*A*) 0 μM, (*B*) 25 μM, (*C*) 60 μM, and (*D*) 160 μM of unlabeled Cby at 25°C; 100 mM NaCl was added to the buffer to minimize the effect of nonspecific binding. Assigned residues that display the most significant peak broadening upon binding are labeled.

different conformations. Upon binding to a target, disordered protein can undergo disorder-to-order transition, and this process is accompanied by a significant decrease in conformational entropy (Dyson and Wright 2002; Fuxreiter et al. 2004; Tompa 2005). The coupling of folding and binding events renders the protein–protein interaction low in binding affinity and yet highly specific (Wright and Dyson 1999; Dyson and Wright 2002), which may have important functional implications in cell signaling and regulation.

On the other hand, instead of adopting fully random conformations, many disordered proteins possess significant amounts of residual structure. The conformational propensity in a disordered protein can significantly enhance its binding to the target by decreasing the entropic penalty of association (Fuxreiter et al. 2004). Therefore, the degree of flexibility and the amount of residual structure presence in a disordered protein can directly influence its target recognition and biological function.

To gain a better understanding of the mechanism through which TC-1 interacts with Cby in the Wnt/β-catenin signaling pathway, structural and dynamical knowledge of TC-1 at the molecular level is essential. With this in mind, in this work, we used NMR spectroscopy to extensively characterize the structural and dynamical properties of TC-1. In addition, the regions of TC-1 that are crucial for the interaction with Cby have also been identified.

By using hydrodynamic radius and amide proton temperature gradient measurements, backbone chemical shift analysis, and ^{15}N spin relaxation measurements, we were able to probe both the global and local conformational properties of TC-1. The high compaction factor (0.54) calculated base on the measured R_h indicates that even though TC-1 protein is disordered, it has properties that are substantially different from a fully denatured polypeptide chain and is more similar to a partially folded protein. On the other hand, result of $\Delta\delta_{NH}/\Delta T$ measurements suggest even the disordered state ensemble of TC-1 is relatively compact, it is still not dominated by a single folded structure.

The compactness of the disordered state ensemble can be explained by the relatively high mean hydrophobicity (0.42) and low mean net charge of TC-1 (0.1) compared with other naturally disordered proteins. Based on the sequence analysis of a large number of globular folded and natively unfolded proteins, Uversky et al. (2000) found that a combination of low overall hydrophobicity and large net charge is the signature of naturally disordered proteins. An equation based on these two parameters was proposed to predict whether a protein is natively

unfolded (Uversky et al. 2000). It turns out that the mean hydrophobicity of TC-1 (0.42) is only slightly lower than the minimum mean hydrophobicity (0.45) required for a protein with the same net charge to be in a stable folded form.

Our results of chemical shift analysis and backbone relaxation measurements indicate that a significant amount of residual structure is present in the partially disordered TC-1. Three regions—α1, D44-R53; α2, K58-A64; and α3, D73-T88—with high helical propensity were identified in the C-terminal portion of the protein. To possibly explain the high helical propensity of TC-1 in these regions, the primary sequence of the protein was examined. Figure 1C shows the protein sequence of TC-1 with charged residues underlined. A high density of charged residues is found between residues 41–100. The large ratio of charged residues to hydrophobic residues is one of the reasons this region is predicted to be disordered by PONDR (Romero et al. 2001). However, if examined closely, one can find a consistent pattern of oppositely charged residues in the sequence with either a (i,i + 3) or (i,i + 4) spacing (Supplemental data, Table S1). With model peptide systems, it has been demonstrated that favorable electrostatic interactions between oppositely charged side chains occurring in (i,i + 3) or (i,i + 4) positions can stabilize helical conformation, and the extent of stabilization follows the pattern: i + 4 AB > i + 4 BA ≈ i + 3 AB > i + 3 BA, where A and B represent acidic (Glu, Asp) and basic (Lys, Arg) residues, respectively (Huyghues-Despointes et al. 1993). Therefore, we speculate that the helical structures in the α1, α2, and α3 regions of TC-1 are largely stabilized by these ion–pair and charge–helix dipole interactions. Mutagenesis studies are currently in progress to verify this assumption.

Even though previous studies reported that TC-1 is naturally disordered (Sunde et al. 2004), our results clearly show that the protein adopts relatively compact conformations and has three regions with high-helical propensity in the C-terminal portion of the protein. The following question remains: What role does the transient helical structure of TC-1 play in the interaction with targets? Recently, Jung et al. (2006) demonstrated that TC-1 functions as a positive regulator of the Wnt/β-catenin signaling pathway by interacting with Cby, an inhibitor of the β-catenin–mediated transcription activity (Takemaru et al. 2003). By competing with β-catenin for binding to Cby, TC-1 up-regulates genes such as *LAMC2*, *MMP-7*, *MMP-14*, *CCND1*, *c-Met*, and *CD44* that are known to be involved in aggressive behavior of cancers (Jung et al. 2006). Interestingly, results of pulldown experiments performed on recombinant full-length and deletion mutants of TC-1 and Cby suggest the Cby binds to the C-terminal portion (residue 51–106) of TC-1 (Jung et al. 2006). To investigate whether the transient helical structure of TC-1 is crucial for this protein–protein interaction, we used the chemical shift mapping technique to probe the interaction between TC-1 and Cby. Our result indicates that TC-1 binds to Cby mainly through the transient helical structure in the α1 and α3 regions, as well as the linker between α2 and α3.

Intriguingly, mutagenesis studies by Jung et al. (2006) revealed that while V74E and L96R mutants of TC-1 still interact with Cby, either the K86Q or the T88K mutation would abolish the binding. Based on our structural results, we speculate that the K86Q and the T88K mutations may disrupt the existing ion–pair interactions and cause destabilization of the helical structure in α3, resulting in the inability of TC-1 to bind to Cby. We are currently studying the structural details of the TC-1/Cby complex and the effects of different mutations of TC-1 on the binding with Cby. Structure-guided mutagenesis at specific sites, by which the local structural propensity can be selectively altered, will be performed. Extensive characterization of the interactions between mutational variants of TC-1 and Cby will lead to a better understanding of the relationships between the structural and dynamical features of TC-1 and its function.

Materials and Methods

Protein sample preparation

The pET-15b plasmid containing the human *TC-1* sequence with N-terminal His_6-tag was a gift from Dr. E. Chua (University of Sydney, Australia) (Sunde et al. 2004). The protein was expressed in *Escherichia coli* BL21(DE3) cells. For the ^{15}N-labeled ($^{15}N/^{13}C$-labeled) protein samples, cells were grown at 37°C in 1 L of M9 minimal medium containing 3 g of glucose (^{13}C-glucose) and 1 g of $^{15}NH_4Cl$ and supplemented with 0.1 mM of $CaCl_2$, 1 mM of $MgSO_4$, 10 μg/mL of thiamine, and 10 μg/mL of biotin. Protein overexpression was induced with 0.5 mM of IPTG at A_{590} ~0.7. After IPTG induction, the cells were allowed to grow for 3 h before harvesting. The protein was then purified as previously described (Sunde et al. 2004). However, instead of using HPLC in the final step of the protein purification, the TC-1 protein was purified by FPLC on a Superdex-75 gel filtration column at 4°C, with 10 mM of sodium acetate and 150 mM NaCl as the buffer. The protein yield was ~6 mg per liter of growth. The 20-residue His_6-tag sequence was retained in the NMR sample.

A recombinant full-length human Cby construct was expressed in pDEST17 vector with His_6-tag. Transformed *E. coli* BL21(DE3) cells were grown at 37°C in 1 L of M9 minimal medium containing 3 g of glucose and 1 g of NH_4Cl and supplemented with 0.1 mM of $CaCl_2$, 1 mM of $MgSO_4$, 10 μg/mL of thiamine, and 10 μg/mL of biotin. Protein overexpression was induced with 0.5 mM of IPTG at A_{590} ~0.7. After IPTG induction, the cells were allowed to grow for 3 h before harvesting. Cby formed inclusion bodies and was separated from the soluble materials by centrifugation. The protein was then dissolved in 8 M of urea, 0.1 M Tris HCl (pH 8.0). Materials that remain insoluble were removed by centrifugation. The supernatant was diluted fivefold with 20 mM Tris

HCl (pH 8.0), 5 mM of imidazole, 0.5 M NaCl, and 8 M of urea and was incubated with Ni^{2+} sepharose at room temperature for 2 h. Cby was eluted with 20 mM Tris HCl (pH 8.0), 1 M of imidazole, 0.5 M NaCl, and 8 M of urea. The sample was then dialyzed against 10 mM of sodium acetate (pH 5.0) at 4°C with stepwise decrements in urea concentration (6 M, 4 M, 2 M, and 0 M). The protein yield was ~10 mg per liter of growth. CD spectrum of the purified Cby sample displays a strong positive band at 190 nm and pronounced negative ellipticities at 208 and 222 nm, resembling the CD spectrum of a folded protein with high helical content (data not shown).

NMR spectroscopy

All NMR experiments were performed at 25°C on a Varian Inova 600-MHz spectrometer equipped with an xyz-gradient triple resonance probe. A 0.12 mM of $^{15}N/^{13}C$-labeled TC-1 sample in 10 mM sodium acetate buffer at pH 5.0 was used to record all heteronuclear triple-resonance experiments, including HNCACB, CBCA(CO)NNH, CCC-TOCSY, HN(CA)CO, and HNCO for the backbone resonance assignments (Sattler et al. 1999). All chemical shifts were referenced to the internal DSS (2,2-dimethyl-2-silapentane-5-sulfonate) signal (Wishart et al. 1995).

^{1}H-^{15}N HSQC spectra of a 0.2 mM ^{15}N-labeled TC-1 sample in 10 mM of sodium acetate buffer (pH 5.0) were recorded at 5°C, 10°C, 15°C, 20°C, 25°C, 30°C, and 35°C. The temperature gradients of amide proton chemical shifts ($\Delta\delta_{NH}/\Delta T$) and the errors were calculated based on the best fits to the experimental data.

For the backbone ^{15}N spin relaxation measurements, a 0.3 mM ^{15}N-labeled TC-1 sample in 10 mM of sodium acetate buffer at pH 5.0 was used. R_1 and $R_{1\rho}$ experiments were performed with 10 relaxation delays. For the R_1 experiment, delay times of 10, 50, 100 (duplicate), 160, 220, 280, 360, 440 (duplicate), 530, and 640 ms were used, while for the $R_{1\rho}$ experiment, delay times of 10, 20 (duplicate), 30, 40, 50, 70, 90, 110 (duplicate), 130, and 150 ms were used. The ^{15}N R_2 value of each assigned residue was then calculated on the basis of the observed R_1, $R_{1\rho}$, offset between the resonance and the carrier frequency ($\Delta\omega$) in Hz, and the spin-lock rf field ($B_{SL} = 1.6$ kHz) (Davis et al. 1994),

$$R_{1\rho} = R_1\cos^2\theta + R_2\sin^2\theta, \text{ where } \tan\theta = \frac{B_{SL}}{\Delta\omega}. \quad (1)$$

Steady-state ^{1}H-^{15}N *NOE* values were determined from spectra recorded in the presence and the absence of ^{1}H saturation. A 7-s delay between scans followed by a 5-s period of saturation was used to record *NOE* spectrum with proton saturation. For the *NOE* spectrum recorded without saturation, 12-s delay between scans was used. All R_1, $R_{1\rho}$, and ^{1}H-^{15}N *NOE* spectra were recorded at 25°C utilizing 128 × 513 complex points in t_1 and t_2, respectively, and spectral widths of 8003 and 1215 Hz for ^{1}H (F_2) and ^{15}N (F_1), respectively.

PFG-NMR experiments were performed using the water-suppressed LED pulse sequence (Altieri et al. 1995) on the same sample used for the ^{15}N spin relaxation measurements. To enable the hydrodynamic radius calculation, 1,4-dioxane (9 mM) was added to the protein solution as a reference molecule (Wilkins et al. 1999). Thirteen different gradient strengths (G) were used in each measurement with the strongest gradient strength leading to ~60% decay in the protein signals. The experiment was repeated three times for the error estimation. Intensities (I) of the signals from protein and dioxane were fitted to a function of G,

$$I(G) = Ae^{-DG^2}, \quad (2)$$

where D is the signal decaying rate proportional to the diffusion coefficient. The hydrodynamic radius of the protein (R_h) was determined from the ratio between the decaying rates of the protein and dioxane signals (Wilkins et al. 1999), where

$$R_h = \frac{D(dioxane)}{D(protein)} \times 2.12 \text{ Å}. \quad (3)$$

Data processing and analysis

All data sets were processed using NMRPipe (Delaglio et al. 1995), and the spectra were analyzed with NMRView (Johnson 2004). ^{15}N R_1, $R_{1\rho}$ values of each residue were obtained by fitting the cross-peak intensities to a single exponential decay function. Errors of the relaxation rates were estimated based on the deviations of experimental data from the best-fit decay curves. Duplicate measurements were used to verify the error estimations. The values of *NOE* were determined by the ratios of the peak intensities in the presence and the absence of proton saturation, while the errors were estimated on the basis of the signal-to-noise ratios in the spectra recorded.

Data bank accession code

The chemical shift assignment of TC-1 has been deposited in BioMagResBank (BMRB) with the accession number 15141.

Electronic supplemental material

The Electronic supplemental material contains the list of ion-pairs that may stabilize the helical structure (Table S1).

Acknowledgments

We thank Dr. Elizabeth Chua (University of Sydney) for providing the TC-1 expression plasmid and Dr. Eleanore Liong (University of Sydney) for many helpful discussions on the TC-1 expression and purification. We also thank Dr. Gary Shaw (University of Western Ontario) for his valuable comments on the manuscript. This work was supported by an operating grant and a resource grant from the Canadian Institutes of Health Research (CIHR). W.Y.C. is the recipient of a CIHR New Investigator Award and an Ontario Early Researcher Award.

References

Alexandrescu, A.T. and Shortle, D. 1994. Backbone dynamics of a highly disordered 131 residue fragment of staphylococcal nuclease. *J. Mol. Biol.* **242:** 527–546.

Altieri, A.S., Hinton, D.P., and Byrd, R.A. 1995. Association of biomolecular systems via pulsed field gradient NMR self-diffusion measurements. *J. Am. Chem. Soc.* **117:** 7566–7567.

Andersen, N.H., Neidigh, J.W., Harris, S.M., Lee, G.M., Liu, Z., and Tong, H. 1997. Extracting information from the temperature gradients of polypeptide NH chemical shifts. 1. The importance of conformational averaging. *J. Am. Chem. Soc.* **119:** 8457–8561.

Bracken, C. 2001. NMR spin relaxation methods for characterization of disorder and folding in proteins. *J. Mol. Graph. Model.* **19:** 3–12.

Choy, W.Y. and Forman-Kay, J.D. 2001. Calculation of ensembles of structures representing the unfolded state of an SH3 domain. *J. Mol. Biol.* **308:** 1011–1032.

Choy, W.Y. and Kay, L.E. 2003. Probing residual interactions in unfolded protein states using NMR spin relaxation techniques: An application to Δ131Δ. *J. Am. Chem. Soc.* **125:** 11988–11992.

Choy, W.Y., Shortle, D., and Kay, L.E. 2003. Side chain dynamics in unfolded protein states: An NMR based ^{2}H spin relaxation study of Δ131Δ. *J. Am. Chem. Soc.* **125:** 1748–1758.

Chua, E.L., Young, L., Wu, W.M., Turtle, J.R., and Dong, Q. 2000. Cloning of TC-1 (C8orf4), a novel gene found to be overexpressed in thyroid cancer. *Genomics* **69:** 342–347.

Davis, D.G., Perlman, M.E., and London, R.E. 1994. Direct measurements of the dissociation-rate constant for inhibitor-enzyme complexes via the T_1 ρ and T_2 (CPMG) methods. *J. Magn. Reson. B.* **104:** 266–275.

Delaglio, F., Grzesiek, S., Vuister, G.W., Zhu, G., Pfeifer, J., and Bax, A. 1995. NMRPipe: A multidimensional spectral processing system based on UNIX pipes. *J. Biomol. NMR* **6:** 277–293.

Dyson, H.J. and Wright, P.E. 2001. Nuclear magnetic resonance methods for elucidation of structure and dynamics in disordered states. *Methods Enzymol.* **339:** 258–270.

Dyson, H.J. and Wright, P.E. 2002. Coupling of folding and binding for unstructured proteins. *Curr. Opin. Struct. Biol.* **12:** 54–60.

Dyson, H.J. and Wright, P.E. 2004. Unfolded proteins and protein folding studied by NMR. *Chem. Rev.* **104:** 3607–3622.

Fuxreiter, M., Simon, I., Friedrich, P., and Tompa, P. 2004. Preformed structural elements feature in partner recognition by intrinsically unstructured proteins. *J. Mol. Biol.* **338:** 1015–1026.

Giles, R.H., van Es, J.H., and Clevers, H. 2003. Caught up in a Wnt storm: Wnt signaling in cancer. *Biochim. Biophys. Acta* **1653:** 1–24.

Gordon, M.D. and Nusse, R. 2006. Wnt signaling: Multiple pathways, multiple receptors, and multiple transcription factors. *J. Biol. Chem.* **281:** 22429–22433.

Huyghues-Despointes, B.M.P., Scholtz, J.M., and Baldwin, R.L. 1993. Helical peptides with three pairs of Asp-Arg and Glu-Arg residues in different orientations and spacings. *Protein Sci.* **2:** 80–85.

Iakoucheva, L.M., Brown, C.J., Lawson, J.D., Obradovic, Z., and Dunker, A.K. 2002. Intrinsic disorder in cell-signaling and cancer-associated proteins. *J. Mol. Biol.* **323:** 573–584.

Johnson, B.A. 2004. Using NMRView to visualize and analyze the NMR spectra of macromolecules. *Methods Mol. Biol.* **278:** 313–352.

Jung, Y., Bang, S., Choi, K., Kim, E., Kim, Y., Kim, J., Park, J., Koo, H., Moon, R.T., Song, K., et al. 2006. TC1 (C8orf4) enhances the Wnt/β-catenin pathway by relieving antagonistic activity of Chibby. *Cancer Res.* **66:** 723–728.

Kim, B., Bang, S., Lee, S., Kim, S., Jung, Y., Lee, C., Choi, K., Lee, S.G., Lee, K., Lee, Y., et al. 2003. Expression profiling and subtype-specific expression of stomach cancer. *Cancer Res.* **63:** 8248–8255.

Kim, B., Koo, H., Yang, S., Bang, S., Jung, Y., Kim, Y., Kim, J., Park, J., Moon, R.T., Song, K., et al. 2006. TC1(C8orf4) correlates with Wnt/β-catenin target genes and aggressive biological behavior in gastric cancer. *Clin. Cancer Res.* **12:** 3541–3548.

Liu, J., Perumal, N.B., Oldfield, C.J., Su, E.W., Uversky, V.N., and Dunker, A.K. 2006. Intrinsic disorder in transcription factors. *Biochemistry* **45:** 6873–6888.

Marsh, J.A., Singh, V.K., Jia, Z., and Forman-Kay, J.D. 2006. Sensitivity of secondary structure propensities to sequence differences between α- and γ-synuclein: Implications for fibrillation. *Protein Sci.* **15:** 2795–2804.

Merutka, G., Dyson, H.J., and Wright, P.E. 1995. ''Random coil'' ^{1}H chemical shifts obtained as a function of temperature and trifluoroethanol concentration for the peptide series GGXGG. *J. Biomol. NMR* **5:** 14–24.

Polakis, P. 2000. Wnt signaling and cancer. *Genes & Dev.* **14:** 1837–1851.

Romero, P., Obradovic, Z., Li, X., Garner, E., Brown, C., and Dunker, A.K. 2001. Sequence complexity of disordered protein. *Proteins* **42:** 38–48.

Sattler, M., Schleucher, J., and Griesinger, C. 1999. Heteronuclear multidimensional NMR experiments for the structure determination of proteins in solution employing pulsed field gradients. *Prog. Nucl. Magn. Reson. Spec.* **34:** 93–158.

Sugase, K., Dyson, H.J., and Wright, P.E. 2007. Mechanism of coupled folding and binding of an intrinsically disordered protein. *Nature* **447:** 1021–1025.

Sunde, M., McGrath, K.C., Young, L., Matthews, J.M., Chua, E.L., Mackay, J.P., and Death, A.K. 2004. TC-1 is a novel tumorigenic and natively disordered protein associated with thyroid cancer. *Cancer Res.* **64:** 2766–2773.

Takemaru, K., Yamaguchi, S., Lee, Y.S., Zhang, Y., Carthew, R.W., and Moon, R.T. 2003. Chibby, a nuclear β-catenin-associated antagonist of the Wnt/Wingless pathway. *Nature* **422:** 905–909.

Tompa, P. 2005. The interplay between structure and function in intrinsically unstructured proteins. *FEBS Lett.* **579:** 3346–3354.

Uversky, V.N., Gillespie, J.R., and Fink, A.L. 2000. Why are ''natively unfolded'' proteins unstructured under physiologic conditions? *Proteins* **41:** 415–427.

Wilkins, D.K., Grimshaw, S.B., Receveur, V., Dobson, C.M., Jones, J.A., and Smith, L.J. 1999. Hydrodynamic radii of native and denatured proteins measured by pulse field gradient NMR techniques. *Biochemistry* **38:** 16424–16431.

Wishart, D.S., Bigam, C.G., Yao, J., Abilldgaard, F., Dyson, H.J., Markley, J.L., and Sykes, B.D. 1995. ^{1}H, ^{13}C, ^{15}N chemical shift referencing in biomolecular NMR. *J. Biomol. NMR* **6:** 135–140.

Wright, P.E. and Dyson, H.J. 1999. Intrinsically unstructured proteins: Re-assessing the protein structure-function paradigm. *J. Mol. Biol.* **293:** 321–331.

Yang, Z.Q., Streicher, K.L., Ray, M.E., Abrams, J., and Ethier, S.P. 2006. Multiple interacting oncogenes on the 8p11-p12 amplicon in human breast cancer. *Cancer Res.* **66:** 11632–11643.

Zhang, H., Neal, S., and Wishart, D.S. 2003. RefDB: A database of uniformly referenced protein chemical shifts. *J. Biomol. NMR* **25:** 173–195.